The Cryosphere Discuss., 8, 3057–3068, 2014
www.the-cryosphere-discuss.net/8/3057/2014/
doi:10.5194/tcd-8-3057-2014

The Cryosphere Discussions
Open Access

Brief Communication: Trends in sea ice extent north of Svalbard and its impact on cold air outbreaks as observed in spring 2013

A. Tetzlaff[1], C. Lüpkes[1], G. Birnbaum[1], J. Hartmann[1], T. Nygård[2], and T. Vihma[2,3]

[1]Climate Sciences, Alfred-Wegener-Institut Helmholtz-Zentrum für Polar- und Meeresforschung, Bremerhaven, Germany
[2]Meteorological Research, Finnish Meteorological Institute, Helsinki, Finland
[3]Arctic Geophysics, The University Centre in Svalbard, Longyearbyen, Norway

Received: 4 May 2014 – Accepted: 30 May 2014 – Published: 6 June 2014

Correspondence to: A. Tetzlaff (amelie.tetzlaff@awi.de)

Published by Copernicus Publications on behalf of the European Geosciences Union.

Abstract

An analysis of SSM/I satellite data reveals that the Whaler's Bay Polynya north of Svalbard was considerably larger in the last three winters from 2012 to 2014 compared to the previous 20 years. This increased polynya size leads to strong atmospheric convection during cold air outbreaks in a region north of Svalbard that typically was ice covered in the last decades. The change in ice cover can strongly influence local temperature conditions. Dropsonde measurements from March 2013 show that the unusual ice conditions generate extreme convective boundary layer heights that are larger than the regional values reported in previous studies.

1 Introduction

Arctic sea ice extent has strongly decreased in the last decade (Stroeve et al., 2012). This is most pronounced in summer and early autumn, during the period of sea ice melt, but there is increasing evidence for a negative trend also during the remaining seasons. Cavalieri and Parkinson (2012) show that in March sea ice extent declined by about 3 % per decade from 1979 to 2010, but with large regional differences. For the Barents and Greenland Sea region they find decline rates exceeding 5 % per decade in winter and spring.

The latter regions are of special interest for ocean–atmosphere interactions due to frequent cold air outbreaks (CAO) (e.g. Kolstad and Bracegirdle, 2008; Brümmer and Pohlmann, 2000; Chechin et al., 2013; Gryschka et al., 2008) with extremely large energy fluxes between ocean and atmosphere downstream of the ice margin. This means that, even if the number of CAOs remained unchanged, a position change of the ice edge would have a strong impact on the local temperature conditions. This especially holds for the Svalbard archipelago, which is close to the Fram Strait marginal sea ice zone. It has been shown by Ivanov et al. (2012) and Falk-Petersen et al. (2014) that sea ice retreat is visible at the northern boundary of Svalbard by an increase of

TCD
8, 3057–3068, 2014

the "Whaler's Bay Polynya" extent (Fig. 1a). This sensible heat polynya forms due to the West Spitsbergen current that causes upwelling of warm Atlantic water (Aagaard et al., 1987; Ivanov et al., 2012). Based on remote sensing data Ivanov et al. (2012) observed a decrease in the ice concentration north of Svalbard by more than 10 % in the period between 1999 and 2011 compared to the period between 1979 and 1995. They also found an increase in the near-surface air temperatures in the ERA-Interim reanalysis in this area, which is in line with the decreasing ice concentration in the last decade.

In this study we show that the extent of the polynya was even considerably larger in the following winters from 2012 to 2014. In-situ observations based on dropsondes released from the Polar 5 aircraft of the Alfred Wegener Institute demonstrate furthermore the strong impact on convection during CAOs north of Svalbard. We present case studies of two CAOs in March 2013 that are influenced by the increased polynya extent. In addition, we use reanalysis data to analyze the impact of an increased polynya size on local temperature conditions. The evolution of the polynya extent is presented in Sect. 2, followed by the case studies in Sect. 3.

2 Polynya size from 1992 to 2014

The wintertime (JFM) variability of the Whaler's Bay sea ice cover between 1992 and 2014 is studied using daily SSM/I ice concentration data provided by Ifremer/Cersat (http://cersat.ifremer.fr) with a spatial resolution of 12.5 km on the basis of the ASI retrieval algorithm by Spreen et al. (2008).

We calculate the JFM mean ice concentration as in Ivanov et al. (2012) in a region northeast of Svalbard expanding from 15 to 60° E and 81 to 83° N referred to in the following as the Western Nansen Basin (WNB). Although Ivanov et al. (2012) considered the period from November till May and used ice concentration data with 25 km resolution, the two time series of mean ice concentrations show the same general characteristics (see Fig. 1b). We find a 20 year mean of 89.5 ± 4.0 % from 1992 to 2011

TCD
8, 3057–3068, 2014

which compares reasonably well with the value of 87.5 ± 5.0 % by Ivanov et al. (2012) for this period. In the winters of 2012 to 2014, however, there is a sudden decrease of the mean ice concentration to below 70 %, which is more than four standard deviations below the 20 year mean.

Another useful quantity is the polynya length, which is an important factor influencing the evolution of a convective atmospheric boundary layer (ABL) during CAOs. We define the polynya length as the cumulative open water path along the yellow area in Fig. 1a, starting at the northwestern edge of Svalbard. Here, the ice edge is defined at 70 % ice concentration. Daily values of the polynya length are shown in Fig. 1c. In the winters of 1992 to 1998 the polynya length hardly ever exceeded 200 km while lengths exceeding 300 km occured more frequently between 1999 and 2011. As for mean ice concentration, 2012 to 2014 were also exceptional in terms of the polynya length with values exceeding 400 km more than 40 % of the time.

3 Cold air outbreaks north of Svalbard in March 2013

The aircraft campaign STABLE (Spring Time Atmospheric Boundary Layer Experiment) of the Alfred Wegener Institute took place in March 2013, one of the years with an extremely large Whaler's Bay Polynya. During that time, several strong CAOs occurred starting with roll convection over the Whaler's Bay Polynya clearly visible in satellite images (Fig. 2a). The strong convective regime, which is unusual for the region north of Svalbard (e.g. Brümmer and Pohlmann, 2000), could be documented by dropsondes released along flight tracks roughly parallel to the convection rolls. A detailed description of the dropsonde unit can be found in Lampert et al. (2012). In the following we discuss two cases of CAOs causing convection over the polynya area on the basis of the dropsonde measurements.

On 4 March 2013 a CAO developed west of Svalbard over the Fram Strait. It was caused by a strong high pressure system over Greenland and a low pressure channel expanding over the Barents and Kara Seas. Vertical profiles of wind, temperature, and

TCD
8, 3057–3068, 2014

humidity were obtained from six dropsondes released along 5° E in distances of 0.5° latitude (Fig. 2b). We found the typical vertical temperature structure of a convective case with a well mixed layer between the surface and a strong capping inversion together with an increasing temperature and atmospheric boundary layer height with distance from the ice edge. This documents the convective character of the ABL as found earlier during Fram Strait CAOs (Brümmer, 1997; Hartmann et al., 1997; Chechin et al., 2013; Lüpkes and Schlünzen, 1996; Wacker et al., 2005). The vertically averaged ABL potential temperature increased from 243 K at 64 km north of the ice edge by 18 K at 214 km south of it (Fig. 3a). Simultaneously, the boundary layer height increased from 150 m to about 2500 m, which is extremely large for this northern position.

The ABL height in CAOs depends on wind direction and speed, as well as temperature conditions. Another possible reason for the extreme ABL height at this latitude can be found by considering the open water fetch. A rough estimate of the latter can be derived from backward trajectories calculated for a height of 10 m using the HYSPLIT transport and dispersion model by NOAA (Draxler and Rolph, 2013, see Fig. 2b). For the southernmost dropsonde the fetch of 350 km was much larger than just the north-south distance to the ice edge of only 214 km. In this case the fetch is strongly increased due to north-easterly winds in contrast to the usual north-south orientation of CAOs. The large fetch might explain the extreme ABL height that is larger than any value published in the literature for this region. The most comprehensive data set is from Brümmer (1997) who measured boundary layer growth during CAOs in the Fram Strait during the aircraft campaign ARKTIS '93 in March 1993. In that year the ice edge was located at 80° N and the Whaler's Bay Polynya was nearly closed. Comparing our measurements to the ARKTIS '93 results (Fig. 3c), we find that the boundary layer height of 2500 m on 4 March, located at 78.5° N, was larger than in all observed cases during ARKTIS '93. The largest boundary layer height observed by Brümmer (1997) was only about 2100 m at 77.5° N, which is 100 km further to the south.

During another CAO on 26 March 2013 we observed boundary layer heights exceeding 1000 m north of 80° N (Fig. 3b and c). While this value is in the usual range of

TCD
8, 3057–3068, 2014

convective ABL heights during CAOs, it is quite unusal for this northern latitude. In this case north-easterly winds prevailed over the Whaler's Bay Polynya. Eight dropsondes were released during a flight from the north-eastern edge of the polynya towards the region west of Svalbard (Fig. 2a). Here, the mean boundary layer potential temperature increased from 248 K over the pack ice to 257 K at the north-western corner of the Svalbard archipelago (Fig. 3b). The boundary layer height increased from 200 to a maximum of more than 1100 m. West of Svalbard the boundary layer characteristics stayed nearly the same since the fetch did not increase any more due to a more northerly wind direction. It is also visible in Fig. 2a that the backward trajectories agree very well with the observed roll orientation.

The close connection between the polynya and the local temperature in the polynya region can be seen in Fig. 3d. There, we show ERA-Interim (Dee et al., 2011) 2 m air temperatures that are available every six hours to determine the impact of the polynya size on local temperature conditons. The temperature is considered at grid points located north of Svalbard (80.25° N, 12–15° E) and for north-easterly winds (30–60°) only, which are identified from the 10 m wind field of ERA-Interim. The relationship between the JFM mean temperatures during north-easterly winds and the mean polynya length is probably not linear since temperatures will roughly approach the water temperature for larger polynya lengths. Therefore, we calculate the Spearman rank correlation that can be used to test the strength of a non-linear relationship. We find a strong correlation of $r_s = 0.73$, which is in line with the more general findings by Ivanov et al. (2012). Thus, depending on the temperature of the inflowing air masses, near-surface temperatures north of Svalbard can be more than 20 K higher in years with a large polynya extent compared to years with a closed ice cover.

4 Conclusions

There is a strong negative trend in the sea ice cover north of Svalbard. We showed that the extent of the Whaler's Bay Polynya north of Svalbard was much larger in the years

TCD
8, 3057–3068, 2014

2012 to 2014 than ever observed in the previous two decades. The strong atmosphere–ocean interaction above the polynya alters the structure of the atmospheric boundary layer during cold air outbreaks and can have a large impact on the local temperatures around Svalbard. Based on ERA-Interim data within the polynya we found that increased near-surface temperatures in this region are strongly related to a larger polynya extent. In addition, we observed an increase of the potential temperature by 9 K over the open water compared to the pack ice region during a CAO on 26 March 2013 north of Svalbard.

The increased fetch due to the larger polynya extent results in events with strong roll convection in a region with usually stable stratification. We find a large ABL height in a region where such values have never been observed before. Average boundary layer heights north of Svalbard are mostly below 300 m in winter according to an ERA-40 climatology from 1957 to 2002 by Wetzel and Brümmer (2011, their Fig. 7). A large extent of the Whaler's Bay Polynya is, however, a precondition for boundary layer heights exceeding 1000 m north of 80° N during CAO. We observed a maximum boundary layer height of 2500 m in the Fram Strait at 78.5° N which is a large value for this latitude compared to other studies of CAO (Brümmer, 1997; Hartmann et al., 1997). With predictions of a further shrinking Arctic sea ice volume in the next decades (e.g. Overland and Wang, 2013) a large Whaler's Bay Polynya, as observed in 2012 to 2014, might be present more often in the future.

Acknowledgements. This work was partly funded by DFG (grant LU 818/3-1) and the Academy of Finland (grant 259537). We would like to thank M. Maturilli, who was in charge of the dropsonde unit.

References

Aagaard, K., Foldvik, A., and Hillman, S. R.: The West Spitsbergen Current: disposition and water mass transformation, J. Geophys. Res., 92, 3778–3784, doi:10.1029/JC092iC04p03778, 1987. 3059

TCD
8, 3057–3068, 2014

Brümmer, B.: Boundary layer mass, water, and heat budgets in wintertime cold-air outbreaks from the Arctic sea ice, Mon. Weather Rev., 125, 1824–1837, doi:10.1175/1520-0493(1997)125<1824:BLMWAH>2.0.CO;2, 1997. 3061, 3063, 3068

Brümmer, B. and Pohlmann, S.: Wintertime roll and cell convection over Greenland and Barents Sea regions: a climatology, J. Geophys. Res., 105, 15559–15566, doi:10.1029/1999JD900841, 2000. 3058, 3060

Cavalieri, D. J. and Parkinson, C. L.: Arctic sea ice variability and trends, 1979–2010, The Cryosphere, 6, 881–889, doi:10.5194/tc-6-881-2012, 2012. 3058

Chechin, D. G., Lüpkes, C., Repina, I. A., and Gryanik, V. M.: Idealized dry quasi 2-D mesoscale simulations of cold-air outbreaks over the marginal sea ice zone with fine and coarse resolution, J. Geophys. Res., 118, 8787–8813, doi:10.1002/jgrd.50679, 2013. 3058, 3061

Dee, D. P., Uppala, S. M., Simmons, A. J., Berrisford, P., Poli, P., Kobayashi, S., Andrae, U., Balmaseda, A., Balsamo, G., Bauer, P., Bechtold, P., Beljaars, A. C. M., van de Berg, L., Bidlot, J., Bormann, N., Delsol, C., Dragani, R., Fuentes, M., Geer, A. J., Haimberger, L., Healy, S. B., Hersbach, H., Holm, E. V., Isaksen, L., Kallberg, P., Köhler, M., Matricardi, M., McNally, A. P., Monge-Sanz, B. M., Morcrette, J., Park, B., Peubey, C., de Rosnay, P., Tavolate, C., Thepaut, J., and Vitart, F.: The ERA-Interim reanalysis: configuration and performance of the data-assimilation system, Q. J. Roy. Meteor. Soc., 137, 553–597, doi:10.1002/qj.828, 2011. 3062

Draxler, R. and Rolph, G.: HYSPLIT (HYbrid Single-Particle Lagrangian Integrated Trajectory) Model access via NOAA ARL READY Website, available at: http://www.arl.noaa.gov/HYSPLIT.php (last access: 5 June 2014), NOAA Air Resources Laboratory, College Park, MD, 2013. 3061

Falk-Petersen, S., Pavlov, V., Berge, J., Cottier, F., Kovacs, K. M., and Lydersen, C.: At the rainbow's end: high productivity fueled by winter upwelling along an Arctic shelf, Polar Biol., 1–7, doi:10.1007/s00300-014-1482-1, 2014. 3058

Gryschka, M., Drüe, C., Etling, D., and Raasch, S.: On the influence of sea-ice inhomogeneities onto roll convection in cold-air outbreaks, Geophys. Res. Lett., 35, L23804, doi:10.1029/2008GL035845, 2008. 3058

Hartmann, J., Kottmeier, C., and Raasch, S.: Roll vortices and boundary-layer development during a cold air outbreak, Bound.-Lay. Meteorol., 84, 45–65, doi:10.1023/A:1000392931768, 1997. 3061, 3063

TCD
8, 3057–3068, 2014

Ivanov, V. V., Alexeev, V. A., Repina, I., Koldunov, N. V., and Smirnov, A.: Tracing Atlantic Water signature in the Arctic sea ice cover east of Svalbard, Adv. Met., 2012, 201818, doi:10.1155/2012/201818, 2012. 3058, 3059, 3060, 3062, 3066

Kolstad, E. W. and Bracegirdle, T. J.: Marine cold-air outbreaks in the future: an assessment of IPCC AR4 model results for the Northern Hemisphere, Clim. Dynam., 30, 871–885, doi:10.1007/s00382-007-0331-0, 2008. 3058

Lampert, A., Maturilli, M., Ritter, C., Hoffmann, A., Stock, M., Herber, A., Birnbaum, G., Neuber, R., Dethloff, K., Orgis, T., Stone, R., Brauner, R., Kässbohrer, J., Haas, C., Makshtas, A., Sokolov, V., and Liu, P.: The spring-time boundary layer in the Central Arctic observed during PAMARCMiP 2009, Atmosphere, 3, 320–351, doi:10.3390/atmos3030320, 2012. 3060

Lüpkes, C. and Schlünzen, K. H.: Modelling the arctic convective boundary-layer with different turbulence parameterizations, Bound.-Lay. Meteorol., 79, 107–130, doi:10.1007/BF00120077, 1996. 3061

Overland, J. E. and Wang, M.: When will the summer Arctic be nearly sea ice free?, Geophys. Res. Lett., 40, 2097–2101, doi:10.1002/grl.50316, 2013. 3063

Spreen, G., Kaleschke, L., and Heygster, G.: Sea ice remote sensing using AMSR-E 89-GHz channels, J. Geophys. Res., 113, C02S03, doi:10.1029/2005JC003384, 2008. 3059

Stroeve, J., Kattsov, V., Barrett, A., Serreze, M., Pavlova, T., Holland, M., and Meier, W. N.: Trends in Arctic sea ice extent from CMIP5, CMIP3 and observations, Geophys. Res. Lett., 39, L16502, doi:10.1029/2012GL052676, 2012. 3058

Wacker, U., Potty, K. V. J., Lüpkes, C., Hartmann, J., and Raschendorfer, M.: A case study on a Polar cold air outbreak over Fram Strait using a mesoscale weather prediction model, Bound.-Lay. Meteorol., 117, 301–336, doi:10.1007/s10546-005-2189-1, 2005. 3061

Wetzel, C. and Brümmer, B.: An Arctic inversion climatology based on the European Centre Reanalysis ERA-40, Meteorol. Z., 20, 589–600, doi:10.1127/0941-2948/2011/0295, 2011. 3063

TCD
8, 3057–3068, 2014

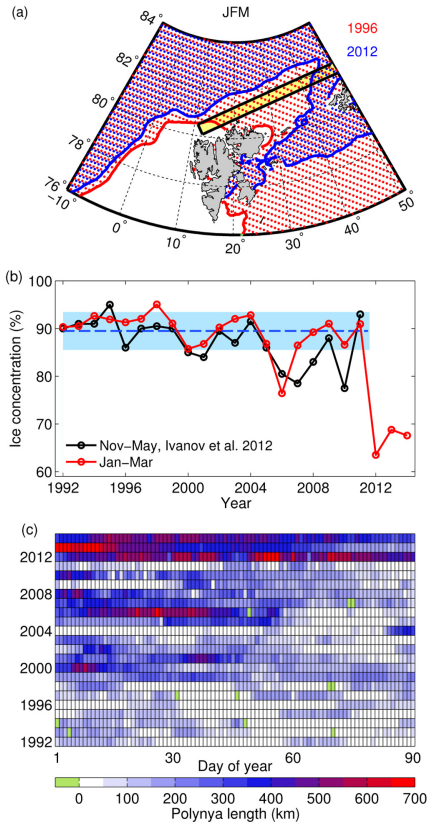

Figure 1. (a) Mean JFM ice edge (based on 70 % SSM/I-ASI ice concentration) in 1996 (red) and 2012 (blue), and area used for calculation of the length of the Whaler's Bay polynya (yellow). **(b)** Time series of the winter mean sea ice concentration in the Western Nansen Basin (WNB, red) with the 20 year mean and one standard deviation (blue). Data from Ivanov et al. (2012) are shown for comparison (black). **(c)** Polynya length for the years 1992 to 2014 as a function of day of the year. Green color denotes missing data.

TCD
8, 3057–3068, 2014

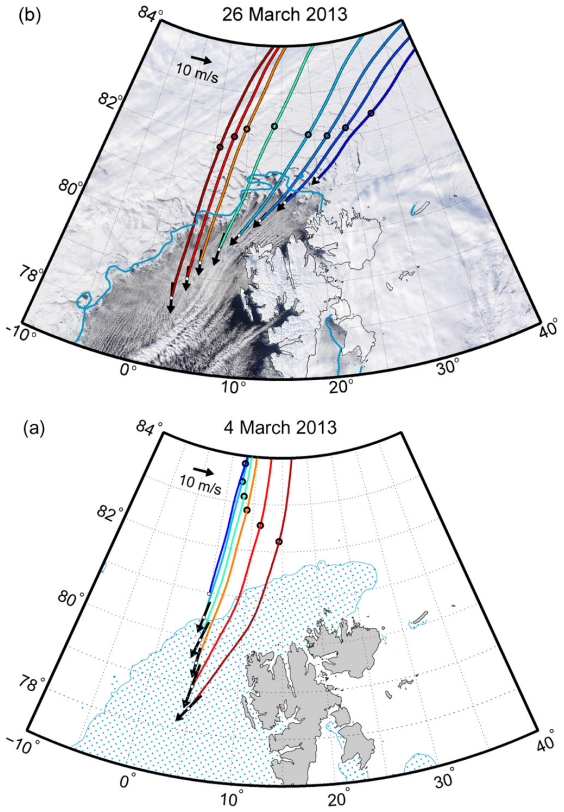

Figure 2. Ice edge based on a 70 % threshold value of the SSM/I-ASI ice concentration during days with cold air outbreaks: 26 March **(a)** and 4 March **(b)** 2013. The arrows denote the vertically averaged wind in the boundary layer at the positions of the dropsondes. The lines are HYSPLIT backward trajectories at 10 m height and the dots mark 10 h. Background of **(a)**: MODIS visible image at 12:45 UTC (http://lance-modis.eosdis.nasa.gov/cgi-bin/imagery/realtime.cgi).

TCD
8, 3057–3068, 2014

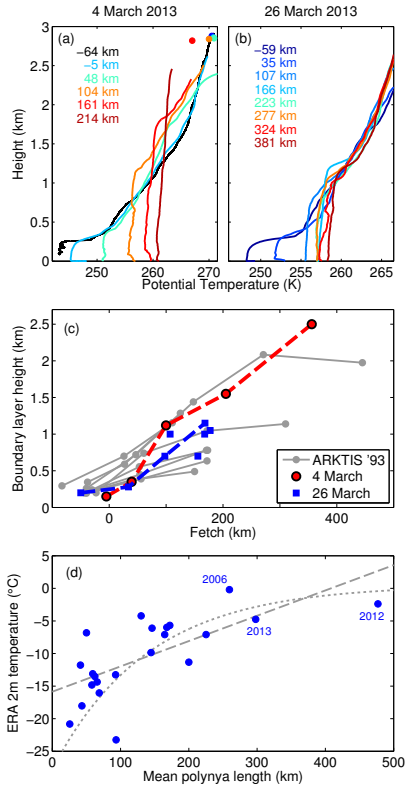

Figure 3. Potential temperature profiles from aircraft (black) and dropsonde (colored) data as a function of distance from the ice edge on 4 March **(a)** and 26 March 2013 **(b)**. The dots are aircraft measurements at the dropsonde release points. **(c)** Boundary layer height for those two days as a function of open water fetch and data from ARKTIS '93 (Brümmer, 1997) for comparison (gray). **(d)** JFM mean ERA-Interim 2 m air temperature north of Svalbard (see text) during times with wind from NE as a function of polynya length from 1992 to 2013 (dots). The lines represent a linear (dashed) and an exponential (dotted) fit.

TCD
8, 3057–3068, 2014